

(π^\pm, xn) reactions

L. B. Church

Department of Chemistry, Reed College, Portland, Oregon 97202

A. A. Caretto, Jr.

Department of Chemistry, Carnegie-Mellon University, Pittsburgh, Pennsylvania 15213

(Received 2 July 1979)

Cross sections for the formation of the ${}^{76}\text{Ge}(\pi^+, xn){}^{76-x}\text{As}$ and the ${}^{76}\text{Se}(\pi^-, xn){}^{76-x}\text{As}$ reaction products were determined for values of x up to six for both 100 and 180 MeV pions. The π^- induced cross sections were consistently higher than those induced by π^+ for all nonzero values of x . Both the π^- and π^+ induced cross sections appear to reach a maximum value when x equals 2 or 3. The results are compared to predictions based on cascade-evaporation calculations and discussed in terms of possible mechanisms. Combining the experimental results for $x = 5$ and 6 with these calculations it was concluded that no significant difference exists in the excitation energy spectrum following π^+ or π^- interaction.

[NUCLEAR REACTIONS ${}^{76}\text{Ge}(\pi^+, xn){}^{76-x}\text{As}$; $E_{\pi^+} = 100$ and 180 MeV; ${}^{76}\text{Se}(\pi^-, xn){}^{76-x}\text{As}$, $E_{\pi^-} = 100$ and 180 MeV; product formation cross sections.]

INTRODUCTION

At incident energies of 100 MeV or more the interaction of π mesons with complex nuclei generally leads to either inelastic scattering or to pion absorption. Inelastic scattering events, with or without pion single charge exchange, normally involve the ejection of the pion together with one or more nucleons on a fast time scale, followed by deexcitation by evaporation of individual nucleons or clusters. In the case of pion absorption, the 140 MeV pion rest mass becomes available for nuclear excitation. Interactions of the type (π, γ) or (π, N) have low probability and therefore absorption processes should in general be expected to lead to the ejection of a considerable array of nucleons or clusters.

The isobar model¹ has been employed to explain both pion absorption as well as pion inelastic scattering. According to this model, for pions with energy below about 300 MeV, the pion and a nucleon form an isobar Δ , with a spin and isospin of $\frac{3}{2}$:



The isobar can either decay,



or scatter with another nucleon,



Pion absorption takes place by reactions (1) and (3). For incident pions in the energy region of 100–200 MeV the pion-absorption mean free path in complex nuclei is about four fm,² roughly comparable to nuclear radii for nuclei around $A = 40$.

Pion absorption, therefore, is an important process, but not the only process that can take place. Pion-nucleon scattering takes place by a combination of interactions (1) and (2) or by nonresonant scattering. The nucleons N'_1 and N'_2 can undergo further scatterings leading to the ejection of various numbers of neutrons, protons, and heavier particles such as deuterons, tritons, and alpha particles, presumably by pickup processes.³ The $(\pi, 2N)$ reaction is generally assumed to be the dominant process for pion absorption.³ This is often followed by (N, xN) cascade reactions and finally deexcitation by evaporation.

The experiments reported here were designed to compare a class of π^+ and π^- induced reactions in which pion absorption provides a major reaction path. Pion absorption becomes the dominant mechanism for reactions of the type (π^\pm, xn) for sufficiently large values of x and not too high values of the incident pion kinetic energy. Specifically, the ${}^{76}\text{Ge}(\pi^+, xn){}^{76-x}\text{As}$ and ${}^{76}\text{Se}(\pi^-, xn){}^{76-x}\text{As}$ reaction cross sections were determined for pions of 100 and 180 MeV and for values of x up to 6, leading to the same series of products. (π, xn) reaction cross sections on ${}^{62}\text{Ni}$ at several energies have been reported by Jackson *et al.*⁴ and are consistent with the results reported here.

The various reaction paths and mechanisms are illustrated in Table I. The product arsenic isotopes, $Z = 33$, thus, can be made by varying contributions of these mechanisms leading to four possible reaction pathways: (i) pion absorption followed by deexcitation by neutron evaporation, (ii) pion single charge exchange followed by deexcitation by neutron evaporation, and (iii) pion inelastic scattering followed by nucleon evapora-

TABLE I. Possible reaction paths and mechanisms.

Path	Mechanism
(i) ${}^{76}_{32}\text{Ge} + \pi^+ \rightarrow {}^{76-x}_{33}\text{As} + xn$	Absorption + neutron evaporation
(ii) ${}^{76}_{32}\text{Ge} + \pi^+ \rightarrow {}^{76-x}_{33}\text{As} + \pi^0 + xn$	Charge exchange + neutron evaporation
(i) ${}^{76}_{34}\text{Se} + \pi^- \rightarrow {}^{76-x}_{33}\text{As} + xn$	Absorption + neutron evaporation
(ii) ${}^{76}_{34}\text{Se} + \pi^- \rightarrow {}^{76-x}_{33}\text{As} + \pi^0 + xn$	Charge exchange + neutron evaporation
(iii) (path A) ${}^{76}_{34}\text{Se} + \pi^- \rightarrow {}^{76-x}_{33}\text{As} + \pi^- + p + (x-1)n$	Inelastic scattering + nucleon evaporation
(iii) (path B) ${}^{76}_{34}\text{Se} + \pi^- \rightarrow {}^{76-x}_{34}\text{Se} + \pi^- + xn$	Inelastic scattering + neutron evaporation followed by decay to observed product
	\downarrow decay \rightarrow ${}^{76-x}_{33}\text{As}$

tion. Mechanism (iii) path A requires the loss of one proton, either in the cascade or by evaporation. Path B leads to the production of neutron deficient target nuclides which subsequently decay in some cases to the observed products. Mechanism (iii) provides reaction paths only in the case of π^- induced reactions.

One of the prime objectives of this study is the comparison of the production cross sections of the same series of nuclides of atomic number Z from an isobaric pair of targets in which π^+ mesons are incident on the $Z-1$ target and π^- mesons incident on the $Z+1$ target. The comparison of the production cross sections of nuclides of atomic number Z lying far from the A of the target in which the absorption mechanism (i) is dominant provides an experimental determination of any differences in the excitation energy spectrum resulting from π^+ or π^- absorption. The yields of neighboring product isotopes are dependent on the excitation energy spectrum following the initial interaction. Such measurements provide a test of predictions of intranuclear cascade calculations which indicate that the residual excitation energy spectrum following π^+ or π^- interactions is independent of the charge of the meson.

EXPERIMENTAL

All irradiations were undertaken at the Los Alamos Meson Physics Facility utilizing the P^3 meson channel. Two pion energies were utilized, 100 and 180 MeV and the channel was tuned to yield a momentum bite of approximately 6% full width at half maximum (FWHM). Throughout the course of these experiments typical meson intensities were about $2 \times 10^8 \pi^+$ /sec and $3 \times 10^7 \pi^-$ /sec. Irradiations were from one to sixteen hours in duration depending on meson charge and energy.

The target materials ${}^{76}\text{Ge}$ and ${}^{76}\text{Se}$ were obtained from Oak Ridge National Laboratory and had en-

richments of 92.82% and 96.88%, respectively. The targets were fabricated by pressing the enriched isotope with high purity aluminum powder and boric acid binders to a pressure of 2750 bars. The resulting 1.5×2.0 cm pellets were self-supporting and were sandwiched between two 12.7 μm thick aluminum guard foils, two 25.4 μm thick aluminum monitor foils, and the entire target assembly wrapped in aluminum. Total target thicknesses ranged from 90 to 300 mg/cm^2 while the thickness of the target element, germanium or selenium, ranged from 26 to 60 mg/cm^2 .

The role of secondary particles contributing to the measured yields from these targets was estimated by irradiating a thick (83 mg/cm^2) naturally isotopic germanium target with π^- mesons. Since the arsenic product nuclides cannot be made by the direct interaction of π^- mesons on germanium, any yield of arsenic products can be attributed to secondary processes. These experiments indicated for the germanium targets employed, that much less than 1% of a typical product cross section could be attributed to secondary processes. It is assumed that the contribution of secondary reactions to the observed products from the selenium targets is comparable. It was not possible to determine this secondary effect experimentally. However, a target thickness study of the (π^-, π^0) reaction in the $A=45$ region indicates a contribution from secondaries of only a few percent for targets up to 50 mg/cm^2 .⁵

All cross sections were monitored by means of the ${}^{27}\text{Al}(\pi^+, x){}^{24}\text{Na}$ reaction for which excitation functions exist.⁶ The specific values of the monitor cross section employed were for π^+ at 100 MeV, 12.0 mb, at 180 MeV, 20.0 mb; for π^- at 100 MeV, 23.5 mb, at 180 MeV, 24.6 mb. The yield of ${}^{24}\text{Na}$ was determined by an assay of the beta activity of the 15 h ${}^{24}\text{Na}$. The germanium and selenium targets were dissolved in appropriate solvents and the radiogenic arsenic separated by suitable chemical procedures⁷ in the presence

TABLE II. Decay properties of product nuclides.

Nuclide	Half-life	Major γ transitions (MeV) and intensities (%)
^{76}As	26.8 h	0.559 (45%)
^{75}As	Stable	
^{74}As	17.8 d	0.596 (60.0%)
^{73}As	80.3 d	0.054 (9%), Ge x rays (100%)
^{72}As	26 h	0.835 (80.0%)
^{71}As	64.8 h	0.175 (91.1%)
^{70}As	53 min	1.040 (81.7%)

of a stable arsenic carrier. The activity of the various nuclides was determined by gamma detection using high-resolution-high-efficiency lithium drifted germanium detectors. Table II lists the gamma transitions observed and their abundances for each of the product nuclides.

RESULTS

Cross sections for the $^{76}\text{Ge}(\pi^+, xn)^{76-x}\text{As}$ reactions and for the $^{76}\text{Se}(\pi^-, xn)^{76-x}\text{As}$ reactions are listed in Table III and plotted in Fig. 1. The results are an average of two or more determinations at each energy for each target element. Values for $x=3$, ^{73}As , were not determined due to the long half-life (76 days) and low detection efficiencies for its radiations. The uncertainties associated with each cross section were determined in the standard manner and take into

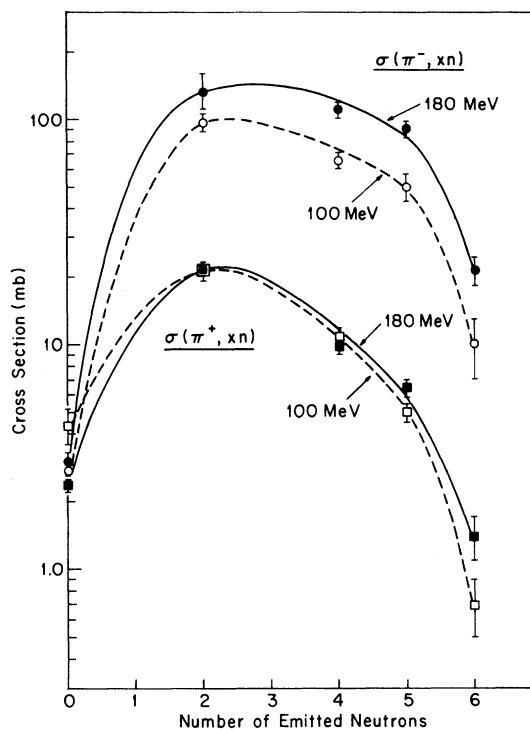


FIG. 1. Cross sections for the $^{76}\text{Ge}(\pi^+, xn)^{76-x}\text{As}$ and $^{76}\text{Se}(\pi^-, xn)^{76-x}\text{As}$ reactions at 100 and 180 MeV vs values of x . Solid lines and solid points, 180 MeV data; dashed lines and open points, 100 MeV data. Circle points, (π^-, xn) reactions; square points, (π^+, xn) reactions.

TABLE III. Experimental and calculated cross sections (mb) for the $^{76}\text{Ge}(\pi^+, xn)^{76-x}\text{As}$ and $^{76}\text{Se}(\pi^-, xn)^{76-x}\text{As}$ reactions.

x	100 MeV		180 MeV	
	Experimental	Calculated	Experimental	Calculated
$^{76}\text{Ge}(\pi^+, xn)^{76-x}\text{As}$				
0	4.4 ± 0.9	8.7 ± 1.6	2.4 ± 0.2	5.4 ± 1.3
1	Stable	16.7 ± 2.2	Stable	8.0 ± 1.6
2	22 ± 2	23.1 ± 2.6	21 ± 2	9.3 ± 1.7
3	N.A.	19.8 ± 2.4	N.A.	11.6 ± 1.9
4	10.5 ± 1.0	7.1 ± 1.4	9.7 ± 0.2	7.2 ± 1.5
5	5.0 ± 0.5	1.8 ± 0.7	6.4 ± 0.3	3.4 ± 1.0
6	0.7 ± 0.2	0.3 ± 0.3	1.4 ± 0.3	0.7 ± 0.4
$^{76}\text{Se}(\pi^-, xn)^{76-x}\text{As}$				
0	<2.7	5.3 ± 1.3	3.0 ± 0.3	4.5 ± 1.2
1	Stable	22.9 ± 2.7	Stable	26.8 ± 2.9
2	97 ± 9	57.4 ± 4.3	130 ± 20	29.5 ± 3.0
3	N.A.	73.4 ± 4.9	N.A.	46.9 ± 3.9
4	65 ± 6	38.2 ± 3.5	110 ± 9	46.4 ± 3.9
5	50 ± 7	12.8 ± 2.0	90 ± 7	29.4 ± 3.1
6	10 ± 3	1.2 ± 0.6	21 ± 3	6.1 ± 1.4

account uncertainties in beam flux measurement, target thickness, detector efficiency, photopeak intensity, irradiation time and counting statistics. The primary contribution to the magnitude of the overall uncertainty was counting statistics, particularly for nuclides with long half-lives, low cross sections, or low detection efficiencies. In an irradiation of about eight hours the beam might be off as much as 5 to 10% of the time and therefore corrections were applied for nonconstancy and nonuniformity of the pion beam.⁸ For this purpose a gamma detector located above the horizontal plane of the pion beam in the P^3 channel was used to detect scattered gamma radiation. The output of this detector was continuously integrated and displayed on a chart recorder. The estimate of the overall experimental uncertainty which is listed in Table III is the larger of either the standard deviation for replicate determinations or the overall uncertainty estimation for individual determinations.

As can be seen from Fig. 1 or Table III, the cross sections of the (π^-, xn) reactions increase with incident pion energy from 100 to 180 MeV; on the other hand, the (π^+, xn) cross sections appear to be rather energy independent. Furthermore, the cross sections of the $^{76}\text{Se}(\pi^-, xn)^{76-x}\text{As}$ reactions are larger than the analogous $^{76}\text{Ge}(\pi^+, xn)^{76-x}\text{As}$ reactions at each energy. In addition, these data suggest that the cross section for these (π^\pm, xn) reactions has a maximum value for x equal to about 2, similar to high energy (p, xn) reactions.⁹ The ratio $\sigma(\pi^-, xn)/\sigma(\pi^+, xn)$ vs x at 100 and 180 MeV is plotted in Fig. 2.

DISCUSSION

In order to understand these data one must take the following facts into account:

- $\sigma(\pi^-, xn) > \sigma(\pi^+, xn)$ for all nonzero values of x and with both 100 and 180 MeV pions.
- For $x > 0$ the (π^-, xn) cross sections are consistently larger at 180 MeV than at 100 MeV, but the (π^+, xn) cross sections appear to have nearly the same values at the two energies except for $x \geq 5$ where the cross sections are larger at 180 MeV than 100 MeV.
- The $\sigma(\pi^-, xn)/\sigma(\pi^+, xn)$ ratio increases with the value of x .

The various mechanisms by which these reactions can take place are illustrated in Table I. Both the (π^+, xn) and (π^-, xn) reactions have the pion absorption (i) and charge exchange (ii) mechanism in common. The (π^-xn) reactions can also take place by inelastic scattering processes (iii). One pathway for these inelastic scattering processes involves the emission of a proton either in the initial cascade or in the evaporation stage.

An alternate inelastic scattering pathway involves the emission of only neutrons in both the cascade and evaporation steps leading to the production of a particle-stable precursor which subsequently beta decays to the observed product.

An estimate of the relative importance of the various reaction paths to a given product can be obtained by comparing the reaction Q values. For the case of $x = 5$ these are given in Table IV. The plausible approximation can be made that the kinetic energy of the outgoing cascade particles, pions and nucleons, in the cases of inelastic scattering or single charge exchange, is about half the incident energy. These are the reaction paths involving negative Q values. Then for the case of 100 MeV incident pions, for large values of x there is only about 10 MeV available for nuclear excitation. Therefore reaction paths involving inelastic scattering and charge exchange have a low probability for large values of x . This condition prevails for $x \geq 5$ and thus pion absorption provides a much more probable reaction path.

Based on the preceding approximation it is reasonable to argue that the contribution to the yield of the $^{76}\text{Ge}(\pi^+, xn)^{76-x}\text{As}$ and $^{76}\text{Se}(\pi^-, xn)^{76-x}\text{As}$ reaction products from absorption processes should increase with increasing values of x . In fact, for $x \geq 5$, absorption should be the dominant mechanism. Conversely, for $x \leq 2$, charge exchange and inelastic scattering become the prime reaction mechanisms since absorption processes will leave the product nucleus with too much excitation energy for the nucleus to deexcite exclusively by gamma emission.

For the cases in which pion absorption is dominant the following interactions should be considered:



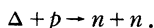
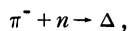
Since the 140 MeV rest mass energy of the pion becomes available, it can be assumed that most pion-absorption processes involve the prompt ejection of at least one nucleon. The experiments

TABLE IV. Reaction Q values.

Reaction	Q (MeV)
$^{76}\text{Ge}(\pi^+, 5n)^{71}\text{As}$	93.91
$^{76}\text{Ge}(\pi^+, \pi^0 5n)^{71}\text{As}$	-41.15
$^{76}\text{Se}(\pi^-, 5n)^{71}\text{As}$	91.89
$^{76}\text{Se}(\pi^-, \pi^0 5n)^{71}\text{As}$	-43.17
$^{76}\text{Se}(\pi^-, \pi^- p 4n)^{71}\text{As}$	-47.06

reported here selected those processes in which the charge of the target nucleus changed by one unit (plus one for $\pi^+ + {}^{76}\text{Ge}$ and minus one for $\pi^- + {}^{76}\text{Se}$). Therefore, reaction (7) above is unlikely since the loss of one proton would produce products other than the arsenic nuclides. Similarly reactions (4) and (6) might lead to further charge change about half the time if a proton is promptly ejected and should contribute nearly equally. One would predict then that π^- absorption should be more probable than π^+ because of the added pathway provided by interaction (5). The experimental results shown in Fig. 2 are consistent with this conclusion.

The dependence of the $\sigma(\pi^-, xn)/\sigma(\pi^+, xn)$ ratio on x must be considered. For $x \geq 5$, absorption is the dominant mechanism and, according to the isobar model, takes place by reactions (1) and (3). Thus the interaction of a π^- meson with a proton and a neutron, reaction (5), might take place by



The elementary π^-n and π^+p cross sections are equal and have a value of 195 mb at the 3-3 resonance while the π^-p and π^+n cross sections are each 70 mb at the same energy. Using these elementary cross sections multiplied by the num-

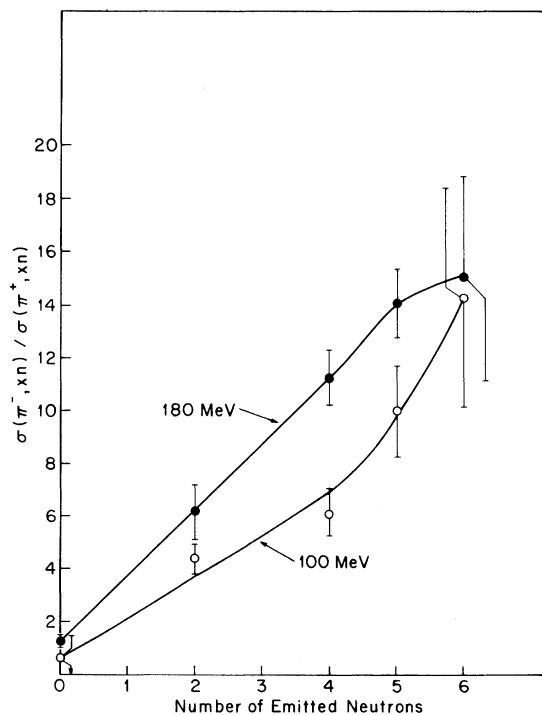


FIG. 2. $\sigma(\pi^-, xn)/\sigma(\pi^+, xn)$ ratio vs x at $E_\pi = 180$ and 100 MeV.

ber of p - p and p - n pairs in ${}^{76}\text{Se}$, and the number of n - n pairs in ${}^{76}\text{Ge}$, the relative probabilities of reactions (4), (5), and (6) can be obtained. The relative probabilities for reactions (4) and (6) were divided by two since it is assumed that on the average at least one nucleon is ejected following absorption and half the time that nucleon could be a proton. Using this crude estimate for the relative probability of π^- absorption vs π^+ absorption, this ratio was calculated to be ~ 9 , in reasonable agreement with the experimental values for large x .

For low values of x where absorption makes an insignificant contribution, if any, the qualitative variation of the $\sigma(\pi^-, xn)/\sigma(\pi^+, xn)$ ratio with x can be explained based on mechanisms (ii) and (iii). The primary π^- interaction can involve π^-p inelastic scattering and charge exchange. In addition π^-n interactions can contribute in inelastic scattering events provided either a proton is subsequently evaporated, or, if only neutrons are evaporated, the resulting nucleus beta decays to the observed product [see Table I mechanism (iii) paths A and B]. Path B does not concern us since the cross sections of ${}^{70}\text{Se}$ and ${}^{71}\text{Se}$ are about 200 times smaller than the corresponding arsenic nuclides¹⁰ and these are the only selenium nuclides which might contribute to the measured cross sections. The cross sections of all the other arsenic nuclides are independent. Furthermore, ${}^{70}\text{As}$ and ${}^{71}\text{As}$ are predominantly produced by absorption processes. Thus mechanism (iii), path B need not be considered further. The primary π^+ interaction involves only π^+n interactions leading to (π^+, π^0p) charge exchange reactions. From consideration of charge independence, $\sigma(\pi^-pp) = \sigma(\pi^+nn)$ and the single collision $\sigma(\pi^-n)$ is almost three times $\sigma(\pi^-p)$. Therefore the $\sigma(\pi^-, xn)/\sigma(\pi^+, xn)$ ratio will increase as a function of x because of the changing probabilities of the various reaction pathways and the resulting differences in residual excitation energy available for nucleon evaporation.

The variation of these (π^\pm, xn) cross sections with energy is illustrated in Fig. 3. The ratio of $\sigma(\pi^-, xn)$ at 180 MeV to $\sigma(\pi^-, xn)$ at 100 MeV is plotted vs x as well as values of the same ratio for the π^+ induced reactions. As can be seen in Fig. 3, the (π^-, xn) cross section energy ratio increases with increasing values of x . A similar trend is noted for the (π^+, xn) reactions. The increase in the cross section with energy for high values of x is again an indication of the importance of pion absorption.

The cross section of the various arsenic product nuclides measured represents a window on the excitation energy developed as a result of the

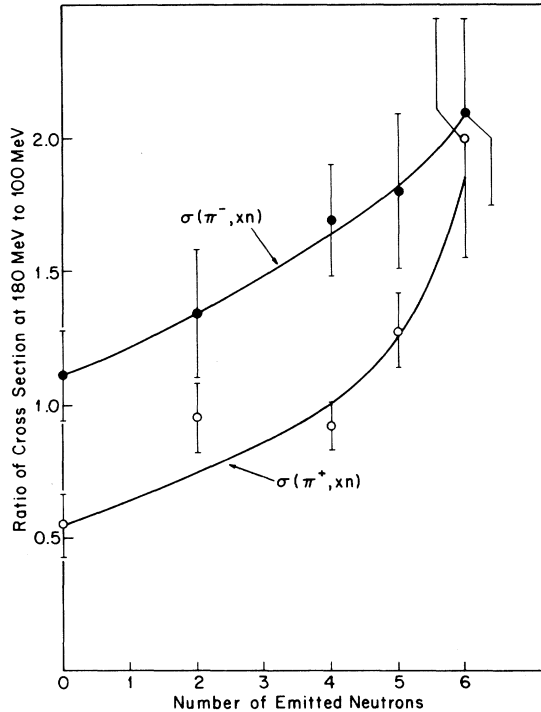


FIG. 3. Ratio of cross section at 180 to 100 MeV vs x for (π^-, xn) and (π^+, xn) reactions.

initial interaction. The variation in the $\sigma(\pi^-, xn)/\sigma(\pi^+, xn)$ ratio with x , based solely on absorption, is determined to a large extent on the probabilities of reactions (4) through (7) and reflects the decrease in the pion-absorption mean free path at 180 MeV as compared with that at 100 MeV. The rapid increase in the $(\pi^+, 5n)$ and $(\pi^+, 6n)$ cross sections with increasing energy are consistent with the absorption mechanism.

These experimental results can be compared with the predictions based on intranuclear cascade and evaporation calculations. For this purpose the ISOBAR version of the VEGAS code^{11,12} was employed together with a modified version of the original evaporation code of Dostrovsky, Fraenkel, and Friedlander.¹³ The cross section for the production of each product nuclide was obtained from both $^{76}\text{Se} + \pi^-$ and $^{76}\text{Ge} + \pi^+$ at both 100 and 180 MeV based on 5000 cascades. Each residual nuclide thus generated was permitted to evaporate neutrons, protons, deuterons, ^3He , tritons, or alpha particles by Monte Carlo evaporation calculations. Reaction paths involving pion absorption, single charge exchange, or inelastic scattering could be identified and thus the relative contribution of the dominant mechanisms could be ascertained.

The results of these VEGAS calculations can be compared to the experimental cross sections

and are listed in Table III. The ratio of experimental cross section to the calculated is generally greater than unity and varies in a random fashion. On a whole the agreement is marginal. Serious discrepancies exist for the 180 MeV π^- data and for large values of x for the other data sets. There is no apparent explanation for this discordance between the calculated and experimental cross sections but it may result from some of the basic assumptions made in the calculation in which these kinds of interactions are treated as a series of independent collisions along a trajectory created by the incident particle. The validity of intranuclear cascade calculations is dependent on the condition that the mean free path of the incident particle be large compared to its de Broglie wavelength and the internucleon distance in the nucleus, but relatively small compared to the nuclear radius. These conditions may be only approximately satisfied. The experimental data reported here represent very restricted processes in which the charge of the target nucleus changes by only one unit. If the calculations improperly simulate the initial pion interaction, one might anticipate large discrepancies in the cross sections for products having very few reaction paths available. The calculated cross sections are of about a factor of 2 larger than the experimental values for the charge exchange products, $x=0$, while the best agreement is observed for values of x between 2 and 4. The experimental cross sections reported here are as much as a factor of 5 larger than the calculated values for $x=5$ and 6. This implies that the calculation underestimates pion-absorption processes.

Although the VEGAS calculation is inconsistent in its prediction of the magnitudes of the cross sections of these (π^\pm, xn) reactions, both the energy dependence and the dependence of the $\sigma(\pi^+, xn)/\sigma(\pi^-, xn)$ ratio with x are roughly predicted. The cross sections versus the number of emitted neutrons x from the VEGAS-evaporation calculations are illustrated in Figs. 4 and 5 for 100 MeV pions. Since the calculation kept track of the reaction path in each case when an arsenic nuclide was the final product, it is possible to calculate the fraction of the cross section of each product which involved pion absorption. These values are also indicated in the figures. For 100 MeV incident pions (see Figs. 4 and 5), the absorption mechanism accounts for 45% of the $(\pi^+, 5n)$ and 67% of the $(\pi^-, 5n)$ cross sections. For $x=6$ the absorption mechanism accounts for virtually 100% of the calculated reaction cross section. These data are summarized in Table V for both 100 and 180 MeV incident pions.

Based only on the absorption mechanism, the

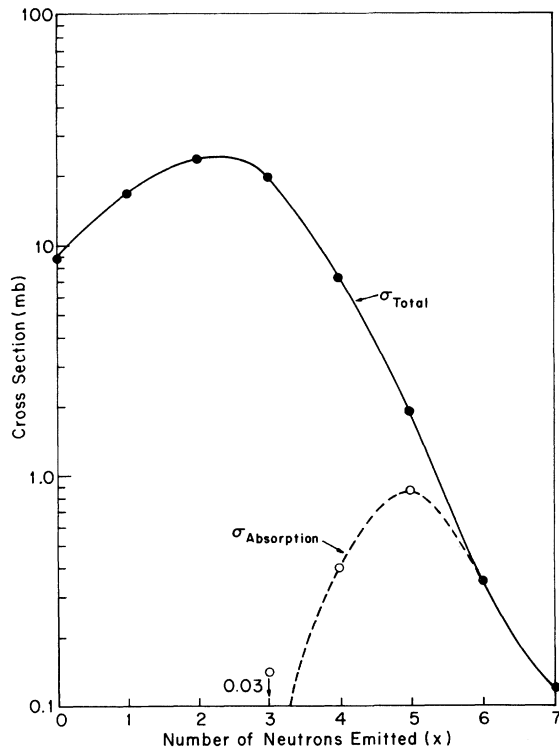
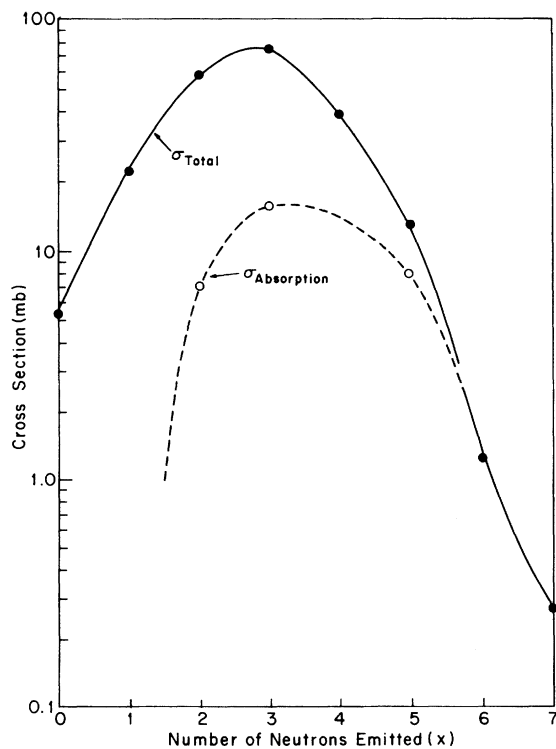
FIG. 4. Calculated $\sigma(\pi^+, xn)$ vs x at $E_{p^+} = 100$ MeV.FIG. 5. Calculated $\sigma(\pi^-, xn)$ vs x at $E_{p^-} = 100$ MeV.

TABLE V. Calculated percent pion absorption.

Reaction	100 MeV	180 MeV
$(\pi^-, 5n)$	62	13
$(\pi^-, 6n)$	100	14
$(\pi^+, 5n)$	47	10
$(\pi^+, 6n)$	100	7

ratio of the yields of two neighboring isotopes produced by π^- mesons to the same ratio resulting from π^+ interaction should reflect the resulting excitation energy spectrum. For example, if the $(\pi^-, 5n)$ and $(\pi^-, 6n)$ reactions both take place by pion absorption, then the ratio of these cross sections depends on the excitation energy spectrum, the neutron binding energy, and the probability of evaporating, only one neutron from the $(\pi^-, 5n)$ product. By comparing the cross section ratio of the same pair of adjacent isotopes from both π^- and π^+ interaction the neutron binding energies cancel out. Thus the ratio

$$\frac{\sigma(\pi^-, 6n)/\sigma(\pi^-, 5n)}{\sigma(\pi^+, 6n)/\sigma(\pi^+, 5n)}$$

should be sensitive only to neutron evaporation probabilities, which in turn depends on the excitation energy spectrum.

This comparison was made for the experimental data for the $x=5$ and $x=6$ cases, and for $x=5$ corrected by the percent of the total cross section which could be accounted for by absorption processes as determined by the VEGAS-evaporation calculations. The assumption is made here that even though the calculated cross sections are not in perfect agreement with the experimental values, the calculated ratio of absorptions to total cross section for each product is approximately correct. The results of this calculation are listed in Table VI along with the experimental value of this ratio prior to correction by percent absorption. These corrected values, 1.1 ± 0.5 for 100 MeV pions and 1.2 ± 0.5 for 180 MeV pions, indicate that, within the experimental uncertainties as well as uncertainties arising from the VEGAS calculation, there is no difference in the excitation energy spectrum resulting from π^+ or π^- interaction with ^{76}Ge or

TABLE VI. Values of the $[\sigma(\pi^-, 6n)/\sigma(\pi^-, 5n)]/[\sigma(\pi^+, 6n)/\sigma(\pi^+, 5n)]$ ratio.

	Ratio	
	100 MeV	180 MeV
Experimental	1.4 ± 0.6	0.8 ± 0.3
Corrected	1.1 ± 0.5	1.2 ± 0.5

^{76}Se , respectively.

The cross sections reported for $x=0$ presumably results from pion single charge exchange interactions. The (π^+, π^0) cross section is lower at 180 MeV (2.4 ± 0.2 mb) than at 100 MeV (4.4 ± 0.9 mb) which is in agreement with multiple scattering theory¹⁴ or the results of coupled channels treatment¹⁵ which predicts a minimum near 180 MeV. Kaufman and Hower¹⁶ calculated the $^{65}\text{Cu}(\pi^-, \pi^0)^{65}\text{Ni}$ excitation function using a Fermi gas model and impulse approximation, and also predicted a minimum at about 200 MeV. However, the intranuclear cascade code ISOBAR appears to predict a maximum near the resonance, based on the calculations reported here as well as other preliminary calculations.¹⁷ Unfortunately only an upper limit could be placed on the value for the cross section of the (π^-, π^0) reaction at 100 MeV. This value is < 2.7 mb at 100 MeV. The measured cross section at 180 MeV (3.0 ± 0.3) mb for the $^{76}\text{Se}(\pi^-, \pi^0)^{76}\text{As}$ reaction would suggest that the (π^-, π^0) single charge exchange cross section, unlike the (π^+, π^0) , is directly proportional to the incident energy.

ACKNOWLEDGMENTS

The authors acknowledge the support which made this work possible. Specifically, L. B. C. expresses appreciation for a M. J. Murdock Trust Grant of the Research Corporation and a summer fellowship from the Northwest College and University Association for Science; A. A. C. expresses appreciation for a National Science Foundation grant. In addition we wish to express appreciation to a number of individuals who helped bring these experiments to fruition. In particular we appreciate the interest and cooperation of Dr. Bruce Dropesky, Dr. Robert Williams, and the LAMPF Nuclear Chemistry group, and Dr. J. N. Ginocchio who provided the results of the VEGAS intranuclear cascade and evaporation calculations. Also many comments and discussions with Dr. Paul Karol were extremely helpful. We thank Mr. James Clark and Mr. Ford Stoll for aid in target preparation. And we particularly wish to thank Mr. Jeffrey Parker for many aspects of extensive assistance during the summer of 1978.

¹R. M. Sternheimer and S. J. Lindenbaum, *Phys. Rev.* **123**, 333 (1961); **109**, 1723 (1958); **105**, 1874 (1957).

²K. G. R. Doss, S. A. Dytman, and R. R. Silbar, *Meson Nuclear Physics-1976*, Proceedings of the International Topical Conference on Meson-Nuclear Physics, edited by P. D. Barnes, R. A. Eisenstein, and L. S. Kisslinger (A.I.P., New York, 1976), p. 344.

³P. D. Barnes, see Ref. 2, pp. 281 and 287.

⁴H. E. Jackson, S. B. Kaufman, D. G. Kovar, L. Meyer-Schützmeister, K. E. Rehm, J. P. Schiffer, S. L. Tabor, S. E. Vigdor, T. P. Wangler, L. L. Rutledge, Jr., R. E. Segal, R. L. Burman, P. A. M. Gram, R. P. Redwine, and M. A. Yates-Williams, *Phys. Rev. C* **18**, 2656 (1978).

⁵R. S. Rundberg, private communication.

⁶Bruce J. Dropesky, private communication.

⁷Collected Radiochemical Procedures, Report No. LA-1721, 4th Edition, Los Alamos Scientific Laboratory, 1976.

⁸Robert A. Williams, private communication.

⁹L. B. Church and A. A. Caretto, Jr., *Phys. Rev.* **178**, 1732 (1969).

¹⁰J. Parker and L. B. Church, unpublished. Cross sections for the production of ^{73}Se and ^{72}Se have been measured using 100 MeV π^- mesons on ^{76}Se . These values were used to predict a cross section for ^{74}Se of less than 2 mb. The cross sections of ^{73}Se and ^{72}Se are also in close agreement with the predictions of intranuclear cascade and evaporation calculations which predict a cross section of 0.2 mb for ^{74}Se and 0.01 mb for ^{70}Se .

¹¹G. D. Harp, K. Chen, G. Friedlander, Z. Fraenkel, and J. M. Miller, *Phys. Rev. C* **8**, 581 (1973); G. D. Harp, *ibid.* **10**, 2387 (1974).

¹²G. N. Ginocchio, *Phys. Rev. C* **17**, 195 (1978).

¹³I. Dostrovsky, Z. Fraenkel, and G. Friedlander, *Phys. Rev.* **116**, 683 (1959).

¹⁴W. R. Gibbs *et al.*, *Phys. Rev. Lett.* **36**, 85 (1971).

¹⁵C. A. Miller and J. E. Spencer, *Phys. Lett.* **53B**, 329 (1974); C. A. Miller and J. E. Spencer, *Ann. Phys.* (N.Y.) **100**, 562 (1976).

¹⁶S. B. Kaufman and C. O. Hower, *Phys. Rev.* **140**, 1272 (1965).

¹⁷J. Ginocchio, private communication.